Warith Scientific Journal of Engineering and Technology

Manuscript 1008

A Wideband Omnidirectional Dual E-Shaped Microstrip Patch Antenna Based on Partial Ground Plane

Fengyu Du

Boning Ren

A Wideband Omnidirectional Dual E-Shaped Microstrip Patch Antenna Based on Partial Ground Plane

Fengyu Du *, **Boning Ren**

School of Measurement-Control Technology and Communications Engineering, Harbin University of Science and Technology, Harbin 150080, China

ABSTRACT

To address the problems of narrow impedance bandwidth in conventional microstrip patch antennas at the 2.4 GHz Bluetooth band and the strong dependence of port matching and radiation efficiency on structural dimensions, this paper investigates the structural design, equivalent-circuit modeling, and test-result analysis of a wideband omnidirectional dual E-shaped microstrip patch antenna based on a partial ground plane. The antenna is fabricated on an F4B dielectric substrate with a relative permittivity of 2.2, a loss tangent of 0.0009, and overall dimensions of 30 mm × 22.5 mm × 1.575 mm. The radiating patch adopts a dual E-shaped slotted configuration, and impedance tuning around 2.4 GHz is realized by combining the microstrip feed line with the partial ground plane. On the basis of the existing parameter analysis, this paper supplements formula-based analyses of the initial microstrip patch dimensions, effective dielectric constant, fringing extension length, input impedance, reflection coefficient, voltage standing wave ratio, equivalent RLC circuit, and efficiency. The antenna structure, equivalent circuit, prototype, S-parameter test curve, radiation pattern, and efficiency curves are inserted into the corresponding analysis positions. The results show that the antenna exhibits good impedance matching over 2.24–2.56 GHz. At the center frequency of 2.4 GHz, the measured reflection coefficient $|S_{11}|$ reaches approximately –43.5 dB, corresponding to a return loss of approximately 43.5 dB. The impedance bandwidth is about 317 MHz, and the fractional bandwidth is about 13.19%. Meanwhile, the gain at 2.4 GHz is approximately 2.41 dBi, the angular width is about 90°, the side-lobe level is about –1.2 dB, and both the radiation efficiency and total efficiency can reach approximately 81%. The study shows that the collaborative design of the dual E-shaped slot and the partial ground plane can effectively broaden the operating bandwidth in the 2.4 GHz Bluetooth band while maintaining a compact structure and convenient fabrication, thereby providing a basis for subsequent performance comparison with a rectangular patch antenna.

Keywords: Dual E-shaped microstrip patch antenna, Partial ground plane, Bluetooth, 2.4 GHz, Impedance matching, Equivalent circuit, S-parameter, Radiation efficiency

Received 19 May 2026; revised 24 June 2026; accepted 24 June 2026.
Available online 3 June 2026

* Corresponding author.
E-mail addresses: m15315337562@163.com (F. Du), 19118603084@163.com (B. Ren).

https://doi.org/10.65892/3079-0697.1008

1. Introduction

With the widespread deployment of Bluetooth, Wi-Fi, ZigBee, and Internet-of-Things terminals in the 2.4 GHz ISM band, terminal antenna designs featuring miniaturization, low cost, and wideband operation have attracted continuous attention. As the key interface between the RF front end and free-space electromagnetic waves, the antenna directly affects wireless-link coverage capability and energy utilization efficiency through its impedance matching, radiation efficiency, radiation-pattern stability, and structural dimensions [1]. Microstrip patch antennas feature a low profile, simple fabrication, and convenient integration with RF circuits, making them suitable for Bluetooth modules, embedded sensor nodes, and compact wireless communication terminals [2].

However, conventional rectangular microstrip patch antennas usually suffer from narrow impedance bandwidth, sensitivity to dielectric substrate and feed position, and insufficient structural tuning freedom. Especially around 2.4 GHz, when the antenna size is constrained by the terminal platform, merely adjusting the length and width of a rectangular patch often makes it difficult to simultaneously satisfy the requirements of resonant frequency, reflection coefficient $|S_{11}|$, radiation efficiency, and radiation-pattern stability. Therefore, improving antenna performance by means of slotted structures, partial ground planes, feed-line dimension adjustment, and equivalent-circuit modeling is a common approach in microstrip antenna optimization [3].

By introducing symmetrical slots into the radiating element, the dual E-shaped patch structure can modify the surface-current path, enhance local electric-field coupling, and introduce a more flexible equivalent inductance and capacitance tuning mechanism near the target band [4]. Compared with an ordinary rectangular patch, the dual E-shaped structure does not simply change the outer contour; instead, it controls the input-impedance trajectory through slot segmentation and path-length extension [5]. When further combined with a partial ground plane, the edge current of the ground plane and the coupling between the feed line and ground plane participate in the resonance formation, which helps reduce the reflection coefficient $|S_{11}|$ and broaden the effective operating bandwidth [6].

Based on this background, this paper takes a wideband omnidirectional dual E-shaped microstrip patch Bluetooth antenna based on a partial ground plane as the research object. The paper is organized as follows. The design considerations are first described with the antenna geometry and main structural parameters. Then, an equivalent RLC model is established to explain the resonance and impedance-matching behavior [7]. Finally, the prototype, S-parameter response, radiation pattern, efficiency, and preliminary comparison with related works are analyzed.

2. Design considerations

The proposed antenna is determined by the coupled effects of the dual E-shaped radiating patch, microstrip feed line, and partial ground plane. Therefore, the design analysis focuses on the substrate, patch dimensions, slot-induced current path, feed-line width, and ground-plane length.

The antenna uses an F4B substrate with dimensions of 30 mm $\times$ 22.5 mm $\times$ 1.575 mm, relative permittivity $\epsilon_r = 2.2$, and loss tangent $\tan\delta = 0.0009$. The radiating patch is printed on the top layer, and the lower layer is a partial ground plane with $Lg = 5$ mm. The main parameters are $L = 30$ mm, $W = 22.5$ mm, $Lp = 20$ mm, $Wp = 10$ mm, $Lf = 10$ mm, $Wf = 3.15$ mm, $Lg = 5$ mm, and $d = 2.22$ mm.

The initial patch dimensions are estimated from the dominant-mode microstrip-patch relations. For a center frequency f_0, the patch width is given by:

$$W_p = \frac{c}{2f_0}\sqrt{\frac{2}{\varepsilon_r + 1}} \tag{1}$$

where c is the speed of light in free space, f_0 is the center frequency, and ϵ_r is the substrate permittivity. The effective dielectric constant is expressed as [8]:

$$\varepsilon_{\text{eff}} = \frac{\varepsilon_r + 1}{2} + \frac{\varepsilon_r - 1}{2}\left(1 + 12\frac{h}{W_p}\right)^{-\frac{1}{2}} \tag{2}$$

where h is the substrate thickness and Wp is the patch width. The fringing-field extension can be calculated by:

$$\frac{\Delta L}{h} = 0.412\frac{(\varepsilon_{\text{eff}} + 0.3)\left(\frac{W_p}{h} + 0.264\right)}{(\varepsilon_{\text{eff}} - 0.258)\left(\frac{W_p}{h} + 0.8\right)} \tag{3}$$

The effective length and resonant frequency are then approximated by:

$$L_{\text{eff}} = L_p + 2\Delta L,\ f_r \approx \frac{c}{2L_{\text{eff}}\sqrt{\varepsilon_{\text{eff}}}} \tag{4}$$

These formulas provide initial values only, because the slots and partial ground plane further change the current path and edge-field distribution [9]. Fig. 1 shows the final three-dimensional structure, top layer, and bottom partial ground plane.

Length-related parameters, including Lp, Lf, Lg, and the slot-induced current path, mainly determine the resonant frequency. Increasing the equivalent electrical length shifts the resonance downward, while decreasing it shifts the resonance upward [10]. The dual E-shaped slots force current to detour along the slot edges, allowing 2.4 GHz resonance within a compact outline [11]. The 5 mm partial ground plane is selected to balance feed return current, impedance matching, and edge radiation [12]. In this configuration, the shortened ground plane modifies the return-current path beneath the microstrip feed and reduces the strong shielding effect of a full ground plane. The truncated ground edge enhances the fringing field around the feed region and introduces additional coupling among the feed line, the dual E-shaped patch, and the ground plane. As a result, the real part of the input impedance can be adjusted toward the 50 Ω condition, while the slot-loaded patch provides the required reactive tuning near 2.4 GHz. If the ground plane is too long, the edge coupling becomes weak and the bandwidth is reduced; if it is too short, excessive radiation from the feed region may deteriorate impedance stability. Therefore, Lg = 5 mm is used as a compromise among impedance matching, bandwidth enhancement, and stable radiation performance.

Width-related parameters, including Wp, Wf, d, and W, mainly affect input impedance, radiation conductance, and local electric-field coupling. A small Wp reduces the effective radiating area, whereas an excessive Wp weakens slot modulation. The slot spacing d controls capacitive coupling between the E-shaped branches, and Wf = 3.15 mm is chosen for approximate 50 Ω feed matching [13].

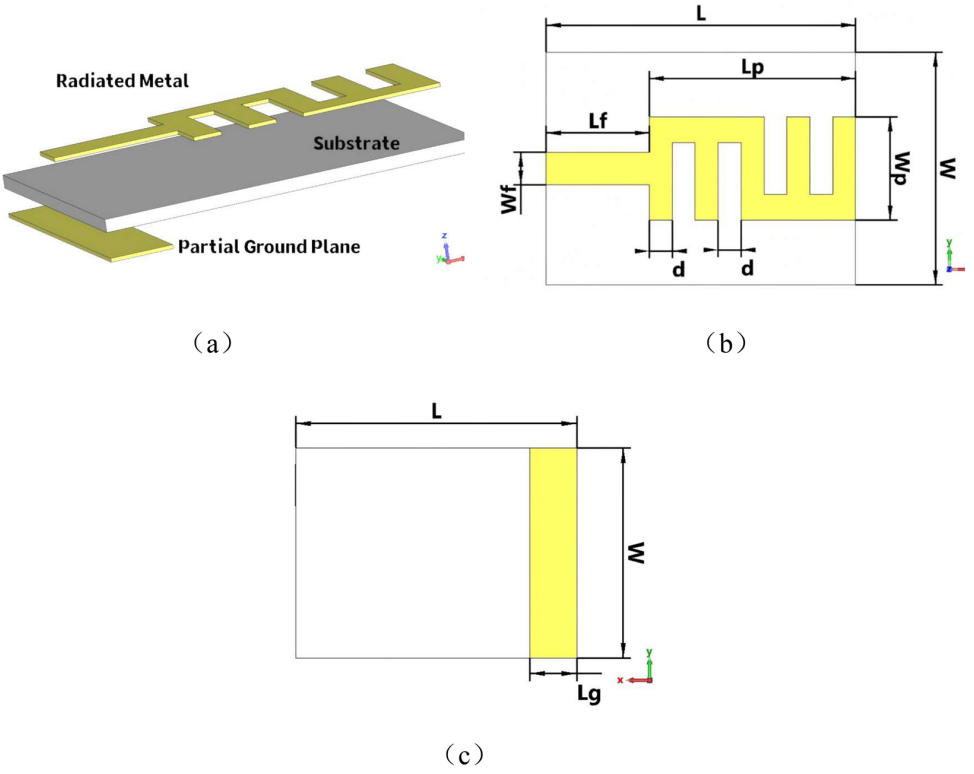

Fig. 1. The proposed antenna structure: (a) 3D view, (b) Top view, and (c) Bottom view, L = 30, W = 22.5, Lp = 20, Wp = 10, Lf = 10, Wf = 3.15, Lg = 5, d = 2.22 (units: mm).

The impedance bandwidth is evaluated from the low- and high-frequency cutoff points as [14]:

$$FBW = \frac{f_H - f_L}{f_0} \times 100\% \tag{5}$$

According to the measured response, the antenna maintains good matching over approximately 2.24–2.56 GHz, corresponding to 317 MHz bandwidth and 13.19% fractional bandwidth [15]. This operating band covers the Bluetooth 2.4 GHz ISM band from 2.400 to 2.4835 GHz, which is used by both Bluetooth Classic and Bluetooth Low Energy systems according to the Bluetooth specification. Therefore, the proposed antenna is suitable for current 2.4 GHz Bluetooth applications rather than being limited to an older Bluetooth version. This verifies the combined tuning effect of the slots, feed line, and partial ground plane.

The microstrip feed line directly excites the dual E-shaped patch and also participates in local electric-field coupling near the input port. If Lf is too short, coupling is insufficient; if it is too long, additional transmission-line effects may appear. In this design, Lf = 10 mm and Wf = 3.15 mm provide a stable feed condition near 2.4 GHz.

3. Antenna equivalent circuit analysis

To explain the 2.4 GHz resonance mechanism, the antenna is modeled as a parallel RLC resonator. In Fig. 2, Rr denotes radiation and loss resistance, Lr represents the magnetic energy associated with the bent current path and feed coupling, and Cr represents the

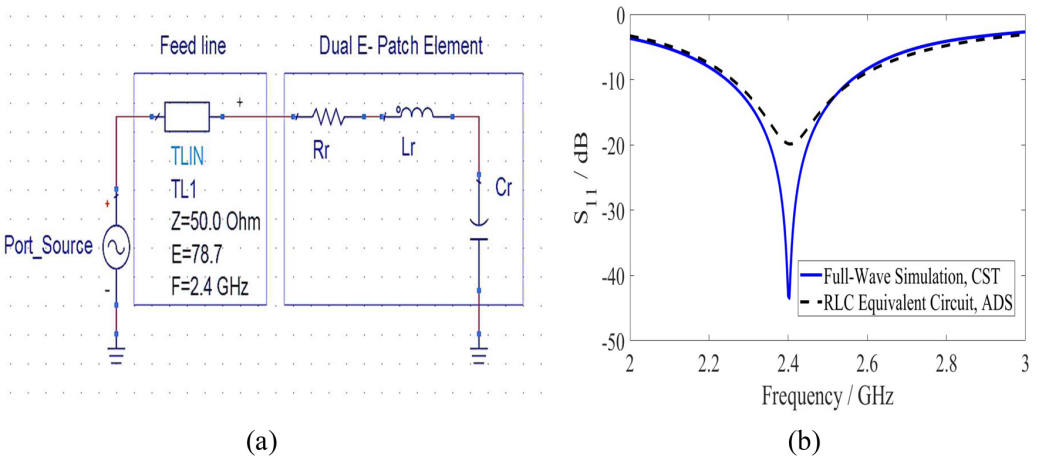

Fig. 2. (a) The proposed antenna's equivalent circuit, and (b) the equivalent-circuit simulated reflection coefficient $|S_{11}|$ in dB.

electric energy associated with the slots and patch-edge field. Fig. 2 gives the equivalent-circuit simulated reflection coefficient $|S_{11}|$ response in dB.

For the equivalent parallel RLC resonator, the input impedance is:

$$Z_{\text{in}} = \left(\frac{1}{R_r} + \frac{1}{j\omega L_r} + j\omega C_r \right)^{-1} \tag{6}$$

where $\omega = 2\pi f$. The equivalent parameters are Rr = 50 Ω, Lr = 25.5 nH, and Cr≈0.172 pF. The corresponding resonant frequency is:

$$f_0 = \frac{1}{2\pi\sqrt{L_r C_r}} \tag{7}$$

Substituting Lr and Cr into equation (7) gives a resonant frequency close to 2.4 GHz, which agrees with the measured and simulated reflection coefficient $|S_{11}|$ results. This confirms that the slot-induced capacitance and current-path inductance form the dominant resonance.

The input impedance can also be derived from the reflection coefficient S_{11} in a 50 Ω system as:

$$Z_{\text{in}} = Z_0 \frac{1 + S_{11}}{1 - S_{11}} \tag{8}$$

When the Smith-chart point approaches the center, the normalized impedance is close to $1 + j_0$ [13]. Thus, the equivalent circuit provides a compact interpretation of the antenna matching behavior near the center frequency.

4. Results analysis

After the design and equivalent-circuit model are established, the fabricated prototype, S-parameter response, far-field pattern, efficiency curves, and comparison table are used to evaluate the antenna performance.

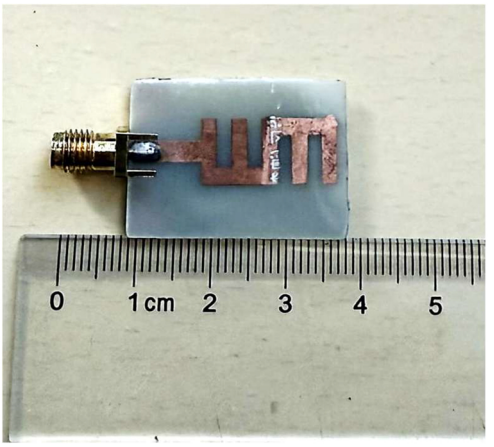

Fig. 3. A prototype of the proposed antenna.

Fig. 3 shows the antenna prototype. The compact PCB structure and SMA connector indicate that the design is compatible with conventional fabrication and measurement procedures.

The reflection coefficient S_{11} is the key indicator of input matching. For antenna input impedance Zin and system impedance Z0, the port reflection coefficient is:

$$\Gamma = \frac{Z_{\text{in}} - Z_0}{Z_{\text{in}} + Z_0} \tag{9}$$

The reflection coefficient magnitude expressed in dB is:

$$S_{11}\,(\text{dB}) = 20\log_{10}|\Gamma| \tag{10}$$

Fig. 4 shows the measured and simulated reflection coefficient $|S_{11}|$ curves in dB.

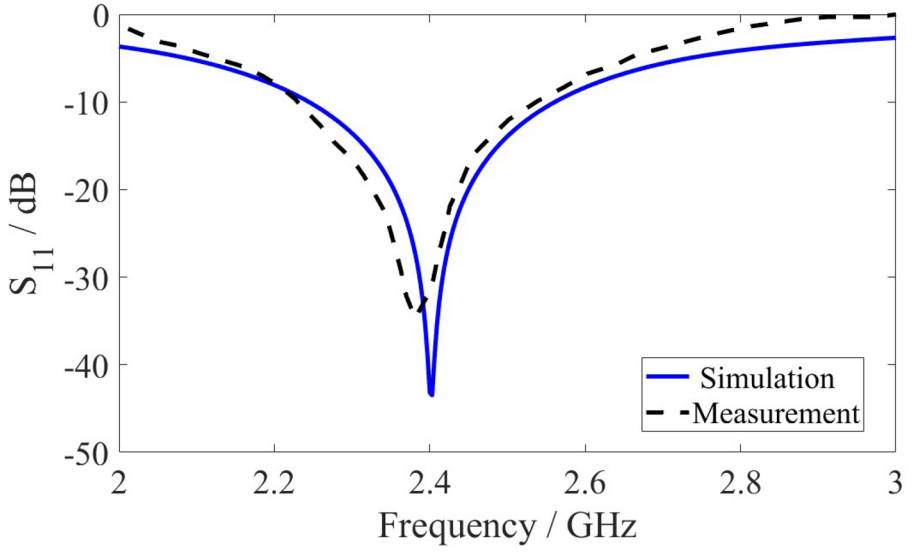

Fig. 4. The measured and simulated reflection coefficient $|S_{11}|$ in dB.

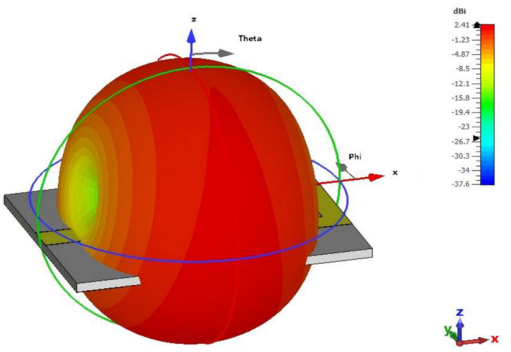

(a)

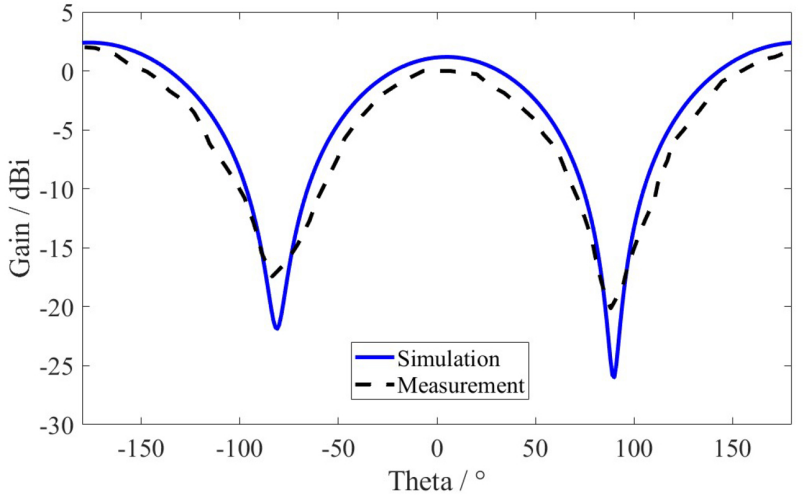

(b)

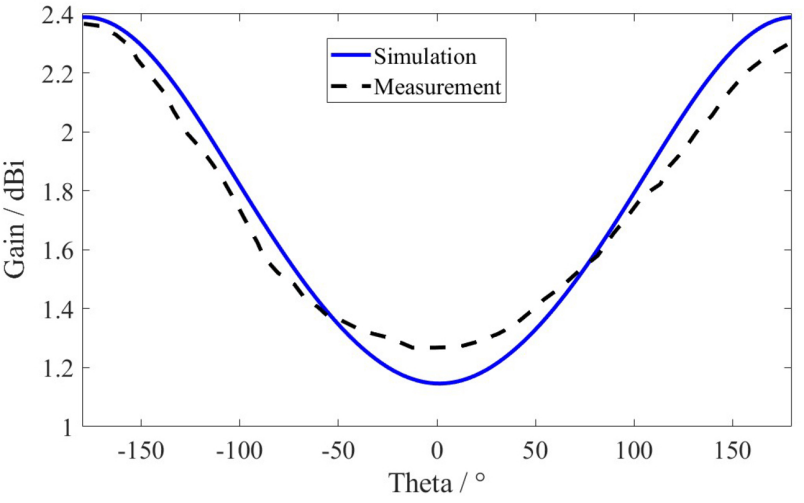

(c)

Fig. 5. The far-field patterns at 2.4 GHz; (a) 3D view, (b) E plane, and (c) H plane.

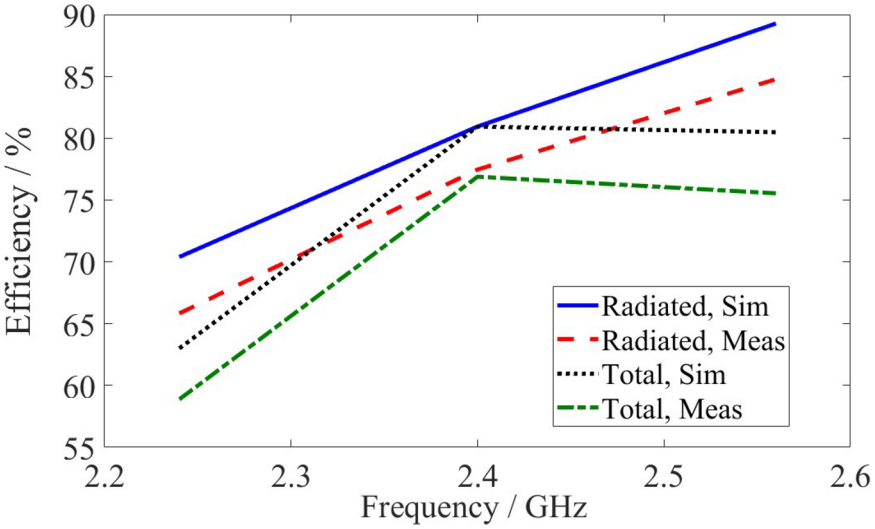

Fig. 6. The measured and simulated efficiencies.

Table 1. Performance comparison between the proposed antenna and related works.

Ref	Dimensions (mm)	Center Frequency (GHz)	Reflection Coefficient $\|S_{11}\|$ (dB)	Realized Gain (dBi)	Efficiency(%)
[16]	58 × 76.74 × 1.6	2.35/2.356	–50.04	3.54	Not reported
[17]	75.85 × 57.23 × 1.6	2.393	–38.86	3.121	Not reported
[18]	40 × 10 × 1.6	2.4	–19.11	1.347	79
[19]	60 × 60 × 1.6	2.4	–25.9	4.66	Not reported
This work	30 × 22.5 × 1.575	2.4	–43.5	2.41	81

As shown in Fig. 4, the antenna has a clear resonant dip near 2.4 GHz, and the measured reflection coefficient $|S_{11}|$ reaches approximately –43.5 dB, corresponding to a return loss of approximately 43.5 dB. The measured –10 dB band is about 2.24–2.56 GHz, corresponding to 317 MHz bandwidth and 13.19% fractional bandwidth. This range fully covers the Bluetooth 2.4 GHz ISM band and provides tolerance for fabrication and installation effects.

The deep $|S_{11}|$ dip results from the joint tuning of the dual E-shaped slots and the partial ground plane. The slots extend the surface-current path and tune local capacitance, while the shortened ground plane enhances feed-edge radiation and adjusts the real part of the input impedance. The low $|S_{11}|$ level also indicates a VSWR close to the matched state around 2.4 GHz.

Gain, radiation pattern, and efficiency are used to evaluate the radiation performance. Fig. 5 shows the far-field patterns at 2.4 GHz, including the 3D radiation pattern, E-plane pattern, and H-plane pattern.

The measured and simulated results show that the antenna achieves a gain of approximately 2.41 dBi at 2.4 GHz, an angular width of about 90°, and a side-lobe level of about –1.2 dB. The pattern exhibits an omnidirectional tendency, which is related to the partial-ground structure and redistributed current on the dual E-shaped patch [6].

Fig. 6 shows the measured and simulated efficiency curves. At 2.4 GHz, both the radiation efficiency and total efficiency are approximately 81%. The close agreement between the two efficiency curves and the low $|S_{11}|$ level indicate that mismatch loss is small and that the F4B substrate, dual E-shaped patch, and partial ground plane form an effective energy-conversion path.

To provide a preliminary comparison with related 2.4 GHz microstrip antennas, Table 1 summarizes the antenna dimensions, center frequency, reflection coefficient $|S_{11}|$, realized gain, and efficiency of the proposed antenna and selected reported designs. Some entries will be further updated after additional literature retrieval.

5. Conclusion

This paper presents a wideband omnidirectional dual E-shaped microstrip patch antenna based on a partial ground plane for 2.4 GHz Bluetooth applications. The dual E-shaped slots, microstrip feed line, and 5 mm partial ground plane jointly control the effective current path, local inductance-capacitance distribution, and input impedance. The equivalent RLC model further explains the resonance and matching behavior near 2.4 GHz.

Measured results show that the antenna operates from approximately 2.24 to 2.56 GHz. At 2.4 GHz, the measured reflection coefficient $|S_{11}|$ is about –43.5 dB, corresponding to a return loss of about 43.5 dB. The bandwidth is about 317 MHz, the fractional bandwidth is 13.19%, the gain is about 2.41 dBi, and both radiation efficiency and total efficiency are approximately 81%. These results demonstrate good impedance matching, acceptable omnidirectional radiation, compact size, and convenient PCB implementation.

Acknowledgements

None.

Conflict of interest

The authors declare no conflict of interest.

Funding

This research received no external funding.

Author contributions

Fengyu Du contributed primarily to the conceptualization, antenna structure design, simulation and measurement analysis, equivalent-circuit interpretation, data organization, and drafting of the manuscript.

Boning Ren contributed to methodology discussion, result validation, manuscript review, and editing. Both authors reviewed and approved the final manuscript.

Data availability statement

Data are available from the corresponding author upon reasonable request.

Ethics statement

This study does not involve human participants or animals.

References

1. Rana MS and Rahman MM. Study of Microstrip Patch Antenna for Wireless Communication System. in 2022 International Conference for Advancement in Technology (ICONAT). Jan. 2022:1–4. doi: 10.1109/ICONAT53423.2022.9726110.
2. Haque MA, Paul LC, Azim R, Mowla MM, Saleh A, Hossain MN. A Modified E-Shaped Microstrip Patch Antenna for C Band Satellite Applications. in 2019 IEEE International Conference on Signal Processing, Information, Communication & Systems (SPICSCON). Nov. 2019:27–31. doi: 10.1109/SPICSCON48833.2019.9065126.
3. Koutinos AG, Zekios CL, Georgakopoulos SV, Kyriacou GA. Increasing the Bandwidth of Antennas Based on the Frequency Pulling Technique: Theoretical Limitations and Practical Considerations. IEEE Trans. Antennas Propag. May 2024;72(5):4064–4076. doi: 10.1109/TAP.2024.3384771.
4. Godaymi Al-Tumah WA, Shaaban RM, Ahmed ZA. A modified E-shaped microstrip patch antenna for dual band in x- and ku-bands applications. J. Phys. Conf. Ser. Jul. 2019;1234(1):012028. doi: 10.1088/1742-6596/1234/1/012028.
5. Khan M, Chowdhury M. Analysis of Modal Excitation in Wideband Slot-Loaded Microstrip Patch Antenna Using Theory of Characteristic Modes. IEEE Trans. Antennas Propag. Nov. 2020;68(11):7618–7623. doi: 10.1109/TAP.2020.2989867.
6. Dinkic J, Stevanovic MN, Djordjevic A. Physical Models for Influence of Substrate Permittivity on the Gain of Microstrip Antennas. IEEE Trans. Antennas Propag. Nov. 2023;71(11):9078–9083. doi: 10.1109/TAP.2023.3310165.
7. Bondala DR, Gopalan A. Simulation and comparison of RF performance of microstrip patch antenna using coaxial probe fed with coplanar waveguide fed on 50 Ω characteristics impedance at 10 GHz. AIP Conf. Proc. May 2023;2655(1):020055. doi: 10.1063/5.0119105.
8. Rano D, Hashmi MS. Determination of Effective Dielectric Constant and Resonant Frequency of Microstrip Patch Antenna with Multilayered Superstrate Structures. in 2019 49th European Microwave Conference (EuMC). Oct. 2019:81–84. doi: 10.23919/EuMC.2019.8910736.
9. Khandelwal SK, Verma A, Yadav A, Goyal A. Comparative Analysis of Various Slot in Patch Antennas: A Review. in 2024 5th International Conference for Emerging Technology (INCET). May 2024:1–5. doi: 10.1109/INCET61516.2024.10593030.
10. Aboserwal N, Ccoillo Ramos NR, Qamar Z, Salazar-Cerreno JL. An Accurate Analytical Model to Calculate the Impedance Bandwidth of a Proximity Coupled Microstrip Patch Antenna (PC-MSPA). IEEE Access. 2020;8:41784–41793. doi: 10.1109/ACCESS.2020.2976750.
11. Latha T, Ram G, Gande AK, Chakravarthy M. Compact Wideband E-Slotted E-Shaped Patch Antenna for Ku-Band Phased Array Applications. IEEE Trans. Aerosp. Electron. Syst. Aug. 2024;60(4):5596–5603. doi: 10.1109/TAES.2024.3374275.
12. Iqbal A *et al.*, Comparative study of micro strip patch antenna for X band using micro strip line feed and coaxial feed. in 2018 International Conference on Engineering and Emerging Technologies (ICEET). Feb. 2018:1–6. doi: 10.1109/ICEET1.2018.8338624.
13. Ida N. The Smith Chart, Impedance Matching, and Transmission Line Circuits. in Engineering Electromagnetics, Cham: Springer International Publishing. 2021:775–812. doi: 10.1007/978-3-030-15557-5_15.
14. Haque MA, Zakariya MA, Paul LC, Nath D, Biswas P, Azim R. Analysis of Slotted E-shaped Microstrip Patch Antenna for Ku Band Applications. in 2021 IEEE 15th Malaysia International Conference on Communication (MICC). Dec. 2021:98–101. doi: 10.1109/MICC53484.2021.9642100.
15. Naik DK, Sahu AK, Parida RK, Raiguru P, Panda DC, Mishra RK. Design of a broadband U-slot loaded E-shaped patch antenna using characteristic mode analysis. AEU - Int. J. Electron. Commun. Sep. 2022;154:154310. doi: 10.1016/j.aeue.2022.154310.
16. Hanashi SMA, Almohamad TA, Aladwani AI, Aziz A, Güneşer MT, Albreem MA. Design and Comparative Analysis of a Microstrip Patch Antenna With Different Feed Technique at 2.4 GHz for Wireless Applications. in 2024 1st International Conference on Logistics (ICL). Aug. 2024:1–6. doi: 10.1109/ICL62932.2024.10788635.
17. Abdulhussein AM, Khidhir AH, Naser AA. 2.4 GHz Microstrip Patch Antenna for S-Band Wireless Communications. J. Phys. Conf. Ser. Dec. 2021;2114(1):012029. doi: 10.1088/1742-6596/2114/1/012029.
18. Islam MS, Islam MT, Ullah MA, Kok Beng G, Amin N, Misran N. A Modified Meander Line Microstrip Patch Antenna With Enhanced Bandwidth for 2.4 GHz ISM-Band Internet of Things (IoT) Applications. IEEE Access. 2019;7:127850–127861. doi: 10.1109/ACCESS.2019.2940049.
19. Demırbas G, Akar E. Design and Interpretation of Microstrip Patch Antenna Operating at 2.4GHz for Wireless WI-FI Application. Avrupa Bilim Ve Teknol. Derg. Mar. 2022;(34):672–675. doi: 10.31590/ejosat.1084151.